

### Central European Journal of Chemistry

# Electrochemical study and MO - modeling of the reduction behaviour of some arylidene substituted derivatives of dibenz [b,e]-thiepin-5,5-dioxide-11-one

#### Research Article

Loredana Predaa, Elena Volanschib\*

<sup>a</sup> Institute of Physical Chemistry "I.G. Murgulescu", Bucharest RO - 060021, Romania

> b Department of Physical Chemistry, University of Bucharest, Bucharest RO - 70346, Romania

#### Received 17 December 2008; Accepted 23 March 2009

Abstract: The electrochemical reduction of four arylidene substituted derivatives of dibenz-[b,e]-thiepin-5,5-dioxide-11- one has been studied by cyclic voltammetry on platinum (Pt) electrode in aprotic media (DMSO), coupled with spectral EPR techniques. From the analysis of cyclic voltammetry experiments, aided by digital simulations using DigiSim software, the kinetic and thermodynamic parameters were evaluated for each system. The electrochemical behaviour is strongly directed by the nature of the arylidene substituents bound to the central heterocycle. The electrochemical investigation and solvent dependent semiempirical modeling using the PM3 hamiltonian in the frame of AMPAC program package allowed a rationalisation of experimental data regarding the electrochemical reduction and the reactivity of the intermediate species involved.

**Keywords:** Electrochemical reduction • Cyclic Voltammetry • EPR-Spectroelectrochemistry • Heterocyclic Sulfones • Solvent dependent MO-modeling

© Versita Warsaw and Springer-Verlag Berlin Heidelberg.

### 1. Introduction

The biological activity of the seven-membered sulfur and oxygen containing heterocycles is well known. Some substituted derivatives of dibenz-[b,e]-thiepine are known for their antihistamine activity, as well as for their central nervous system depressant effects [1,2]. Their use as potential drugs supposes their implication in metabolic redox processes, and therefore a better knowledge of the reduction and oxidation pathways of these compounds, as well as of the reactivity of the intermediate species involved is necessary. Heterogeneous electron transfer (ET) reactions of organic species in solution usually generate a radical ion which may be further involved in follow-up reactions with solution components. If electrochemical methods

are best suited to investigate kinetic and thermodinamic aspects of the ET step, spectral methods (UV-VIS, EPR) and theoretical modeling based on quantum chemistry methods (MO calculations) can furnish information about the reactivity of the intermediates in subsequent reactions and contribute to the molecular understanding of redox processes at a molecular level.

Previous cyclic voltammetry coupled with EPR and UV-VIS spectroelectrochemistry and theoretical modelling studies in the dibenz-[b,e]-thiepin-11-one series [3-7] have pointed out a cleavage of the C-S bond in reduction processes, dependent on the oxidation degree of the heteroatom in the central ring and on the 6-site substituent.

The 6-arylidene dibenz-[b,e]-thiepin-11-one derivatives investigated in our previous work [8] have

revealed different reduction pathways, depending strongly on the substituent in the arylidene moiety, whereas practically no influence was noted for the central heterocycle substituent in site 2.

The aim of the present work is to study four other substituted derivatives in the series, in order to outline the role of the substituent in the arylidene moiety in site 6 on both the reduction mechanism and the reactivity of the intermediates. Cyclic voltammetry with stationary and rotating disc (RDE) electrodes, EPR spectroelectrochemistry and semiempirical (PM3) solvent dependent MO calculations were performed on the four substituted derivatives in Fig. 1. The compounds were synthetised, characterised by the IR and NMR spectra and kindly supplied by the regretted Prof. Perjessy from the Department of Organic Chemistry of the Comenius University in Bratislava, Slovakia.

Figure 1. Structure of the investigated compounds

## 2. Experimental Procedures

The CV measurements were performed with a VOLTALAB-32 electrochemical device. Electrochemical investigations were carried out in an one compartment, three-electrode cell, equipped with a Pt-EDI 101 rotating disc working electrode (RDE) of 2 mm diameter, Pt as a counter electrode and Ag/Ag<sup>+</sup> reference electrode. Experiments were performed at room temperature. Numerical simulations of the voltammograms were performed with the BAS DigiSim simulator 3.03, using the default numerical options with the assumption of planar diffusion and a Butler-Volmer law for the electron transfer.

The anion – radicals for EPR were prepared by *in situ* techniques, using the same solvents

(dimethylsulfoxide, DMSO) and supporting electrolyte (tetra-*n*-butylammonium perchlorate (TBAP, 0.1 M)) as for the electrochemical experiments. The EPR spectra were recorded on a JEOL FA 100 spectrometer in the X-band frequency. The simulation of EPR spectra was performed using the WinSim free software [9]. MO calculations were performed using the PM3 hamiltonian and eigen vector following (EF) optimization algorithm; the model of solvation taken into account was a dielectric continuum model [10] - option COSMO, in the AMPAC program package. Both restricted (ROHF) and unrestricted (UHF) calculations were performed for the open-shell structures. For DMSO a dielectric constant 48.9, refractive index 1.48 and solvatation radius 3 Å were used.

### 3. Results and Discussion

### 3.1. Cyclic voltammetry

Cyclic voltammetry results on compounds **1** and **2** in dimethyl sulfoxide (DMSO) at low and moderate scan rate ( $v = 0.05 \text{ V s}^{-1} - 1 \text{ V s}^{-1}$ ), exhibit in the range + 1 to -1.7 V two successive reduction waves and several anodic peaks. Due to the quite minor differences in the behaviour of both compounds, only the results for compound **1** are presented in Fig. 2a.

The first wave is located at  $E_1^0 = -0.963 \text{ V}$  for **1** and  $E_1^0 = -0.960 \text{ V}$  for **2** and presents a smaller but well shaped anodic counterpart. If the scan is stopped after the first wave, no other oxidation waves are apparent on the anodic scan (Fig. 2b, full line), the ratio  $i_{pa}/i_{pc}$  corresponding to this wave is close to unity in the whole scan rate range, and the peak separation  $E_{pc}-E_{pa}=135-140 \text{ mV}$  at 0.1 V s<sup>-1</sup> for **1** and **2**. This is a direct evidence for a quasi-reversible electrochemical process [11,12], and was assigned to the reduction of the initial compounds **1** and **2**, here after denoted by **A**, to the corresponding anion radicals (**A** + e  $\rightarrow$  **A**<sup>-</sup>).

The second wave, corresponding to the reduction of the anion radical to the dianion ( $\mathbf{A}^- + \mathbf{e} \to \mathbf{A}^2$ ), is located at  $E_{p2} = -1.450$  V at v = 0.1V s<sup>-1</sup> for **1** and  $E_{p2} = -1.480$  V at v = 0.1 V s<sup>-1</sup> for **2** and is irreversible in the entire scan rate range (v = 0.05 V s<sup>-1</sup> – 1 V s<sup>-1</sup>). The peak potential ( $E_p$ ) varies linearly with the logarithm of the scan rate by -74 mV/dec with a peak width  $E_{p/2}$  - $E_p = 68$  mV. These values correspond to an electron transfer followed by a chemical reaction (EC, E - electrochemical and C-chemical) scheme, with a mixed kinetic control by the E and C steps [13,14]. This reaction sequence may be also evidenced by other experimental observations: (I) the appearance of several anodic waves if the scan is stopped after the second wave, suggesting the oxidation

of the products formed after the second reduction step (Fig. 2a full line) and (II) cycling on the extended potential range starting with oxidation, which points out no oxidation waves on the first scan, but appearing on subsequent scans (data not shown).

Possible chemical reactions involving the dianion could be either protonation, the dianion being a strong electrogenerated base (EGB), or cleavage of the C-SO<sub>2</sub> bond, this type of cleavage being frequently signalled for other sulfones [15-20] and also in the dibenz-[b,e] thiepinone series [3-8].

RDE linear voltammetry (Fig. 2a - inset) allows determining the number of electrons, based on the plot of E  $vs \ln((i_1 - i)/i)$  (Eq. 1) [12]:

$$E = E_{1/2} + \frac{RT}{nF} ln(\frac{i_1 - i}{i})$$
 (1)

For compound **1** the slope is 0.028 with N = 13 and r = 0.990 and for compound **2** the slope is 0.027 with N = 10 and r = 0.987 proving the monoelectronicity of the first electron transfer (ET).

The Levich equation (Eq. 2) [12] allowed to determine the diffusion coefficient,  $D_0$ .

$$i_1 = 0.620 nFAD_0^{2/3} \omega^{1/2} v^{-1/6} C_0^*$$
 (2)

where A is the electrode area (cm²),  $\omega$  is the rotating rate (s¹),  $\nu$  = 0.01896 cm² s¹ the kinematic viscosity of the solvent (DMSO) and C₀\* is the bulk substrate concentration (mol cm³). From the plot i₁ = f( $\omega$ ¹¹²) where  $\omega$  varied in the range 100-3200 rpm, the following diffusion coefficients were obtained: D₀ = 9.94×10-6 (cm² s¹1)

(N = 16, r = 0.998) for **1** and  $D_0 = 8.71 \times 10^{-6}$  (cm<sup>2</sup> s<sup>-1</sup>) (N = 20, r = 0.990) for **2**.

For compounds **3** and **4**, generically denoted in the followings by **B**, due to their similar behaviour attesting a minor influence of the methyl substitution in site 2 of the parent heterocycle, the cyclic voltammetry (Fig. 3a) and RDE linear voltammogramms (insert) show also two successive reduction waves, corresponding to the first and respectively second electron transfer ( $\mathbf{B} + \mathbf{e} \to \mathbf{B}^-$  and  $\mathbf{B}^- + \mathbf{e} \to \mathbf{B}^2$ ). If the scan is reversed after the first ET (Fig. 3b - full line), the wave becomes only partially reversible ( $\mathbf{i}_{pa}/\mathbf{i}_{pc}$ << 1) and an anodic wave is apparent on the positive potentials range.

The RDE results indicate, from the slope values in (Eq. 1) (for compound 3 the slopes are 0.027, respectively 0.041 with N = 13 and r = 0.990 respectively N = 10 and r = 0.98 and for compound 4 the slopes are 0.025, respectively 0.051 with N = 18 and r = 0.981 respectively N = 15, r = 0.936), that the electrochemical processes involved are monoelectronic. The diffusion coefficient values (Eq. 2) are: for compound 3,  $D_0 = 7.77 \times 10^{-6}$  (cm² s<sup>-1</sup>) (N = 20, r = 0.995) and for compound 4,  $D_0 = 8.6 \times 10^{-6}$  (cm² s<sup>-1</sup>) (N = 20 r = 0.993).

The first wave located at  $E_1^0 = -0.921$  V for **3** and  $E_1^0 = -0.909$  V for **4**, becomes partially reversible at  $v \ge 0.2$  V s<sup>-1</sup>, indicating a decrease of the radical anion life-time in comparison with that of **1** and **2**. The reversibility of this wave increases with the scan rate, and therefore this wave was associated with a quasi-reversible electrochemical process followed by a chemical reaction (EC process): the peak separation  $E_{pc}$ - $E_{pa} = 140 - 150$  mV at 0.1 V s<sup>-1</sup> for **3** and **4**,  $i_{pa}$ /  $i_{pc}$  increases with v [11,12].

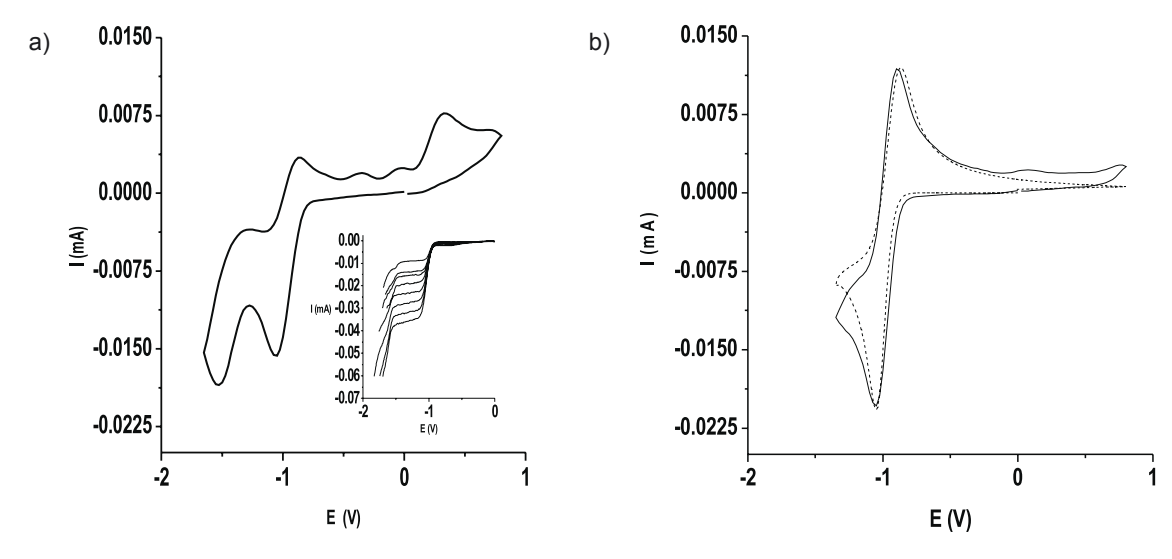
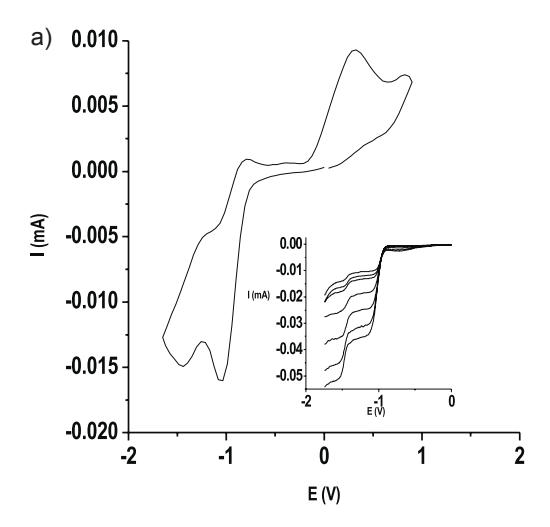


Figure 2. Cyclic voltammetry curves of compound 1 in DMSO, (c = 3×10<sup>-3</sup> M) at v = 0.5 V s<sup>-1</sup>: (a) experimental potential range – 1.8 V to 1 V, starting with reduction; *insert:* RDE curves for rotation rates in the range 200 - 2000 rpm; (b) Cyclic voltammetry curves in the potential range -1.5 V to 1 V (full line) and DigiSim simulation with the parameters in text (dashed line)



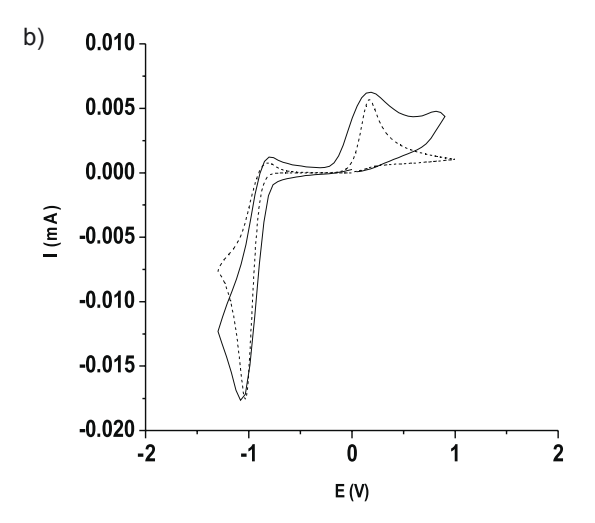


Figure 3. Cyclic voltammetry curves of compound 3 in DMSO, (c = 3×10<sup>3</sup> M) at v = 0.9 V s<sup>-1</sup>: (a) experimental potential range – 1.9 V to 1 V, starting with reduction; insert: RDE curves for rotation rates in the range 200 - 2000 rpm; (b) Cyclic voltammetry curves in the potential range -1.5 V to 1 V (full line) and DigiSim simulation with the parameters in text (dashed line)

The anodic wave observed in the positive range (Fig. 3b – full line) is most probably due to the oxidation of the products formed after the chemical reaction (C) following the first ET.

As noted earlier, for compounds 1 and 2, further support for this assignment is given by cycling on the extended potential range starting with oxidation, which points out no oxidation waves on the first scan, but appearing and increasing in intensity on subsequent scans (data not shown).

The second reduction wave located at  $E_{p2}$  = -1.410 V at 0.1 V s<sup>-1</sup> for **3** and  $E_{p2}$  = -1.364 V at 0.1V s<sup>-1</sup> for **4** is irreversible. The peak potential varies linearly with the logarithm of the scan rate by –58 mV/dec for **3** and by -74 mV/dec for **4** with  $E_{p/2}$ - $E_p$  = 68 mV, corresponding, as noted earlier, to an EC mechanism.

The experimental I - E curves were compared with theoretical curves calculated using the DigiSim 3.03 software for all compounds, in order to estimate the kinetic parameters for the heterogeneous electron transfer and its associated chemical step. The standard potentials and heterogeneous electron transfer rate constants (E $^0$ ,  $k_{\rm s}$ ) for the electrochemical processes, as well as the equilibrium (K $_{\rm eq}$  =  $k_{\rm f}$  /  $k_{\rm b}$ ) and rate constant (k $_{\rm f}$ ) values for the chemical steps, were determined from Digisim simulation and are close to the values deduced from the preliminary analysis of cyclic voltammetry data. For the diffusion coefficients D $_{\rm O}$ , the default values were used (10-5 cm² s-1), very close to the experimental ones in the range  $0.77\times10^{-5}$ –  $0.94\times10^{-5}$  cm² s-1.

The results concerning the electrochemical reduction of compounds 1 and 2, allow to propose the following

mechanistic scheme: the anion radical  $\mathbf{A}$ -obtained at the first reduction step is sufficiently stable to be evidenced by EPR spectroscopy if the potential does exceed that of the first wave (see section 3.2). The second reduction wave is a slow ET followed by a chemical step (EC). Taking into account the previously investigated dibenz - [b,e] - thiepinone derivatives [3-8], the most probable chemical reaction following the second ET is a reductive cleavage of the C - SO<sub>2</sub> bond, leading to the products  $\mathbf{P}$ , which are further oxidized at more positive potentials (Fig. 2a), *i.e.* an EECE reaction sequence:

Simulation of the experimental curves with the DigiSim program is presented in Fig. 2b (dashed line) and supports the proposed mechanism.

In contrast to what was observed for 1 and 2, in the case of 3 and 4, the partial reversibility of the reduction wave indicates that the anion radical  $\mathbf{B}^{-}$  formed in the first ET is partially involved in a chemical step leading to the formation of the products  $\mathbf{P}$ , and in a second ET leading to the dianion  $\mathbf{B}^{2-}$ . Consequently, the life time of the anion radical is shorter (< 3 s) as shown by cyclic voltammetry, and therefore could not be characterised by EPR spectroscopy, not even at continuous electrochemical generation at the potential of the first redox couple by *in situ* techniques. Based on these experimental data, the following mechanistic scheme is proposed for 3 and 4:

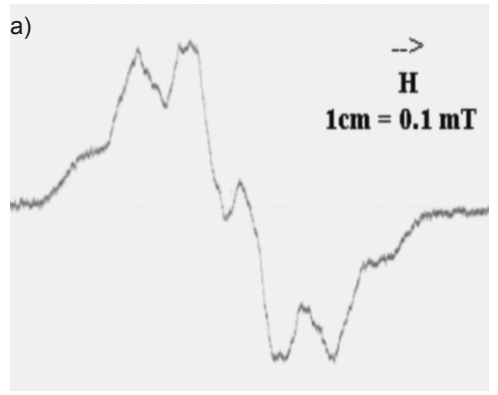




Figure 4. EPR spectrum obtained by in situ electrochemical reduction in DMSO from compound 2 at the potential of the first wave on the voltammogram (a) - experimental; (b) simulated spectra with the hyperfine splittings in the text

The DigiSim simulation with this mechanism is presented in Fig. 3b (dashed line) and supports the proposed ECECE reaction sequence. The Digisim obtained ET-rate constant values,  $k_{s_{,}}$  are quite close to the approximate values evaluated from the cathodic and anodic peak separation,  $\Delta E_{pac}$  [12]. It may be also noted that the  $k_{s}$  values are similar for compounds 1, 2 and respectively 3, 4, meaning that they are not influenced by the nature of the arylidene substituents in site 6 of the central heterocycle.

The standard rate constants obtained for the electron transfers are apparent rate constants, not corrected for double layer effects. Moreover, not all the oxidation waves visible on the extended positive scan could be accounted for, because the program limitation imposes only three ET-steps.

#### 3.2. EPR results

EPR spectra were recorded during the electrochemical reduction in DMSO, in order to identify the paramagnetic intermediates.

In the case of compounds 1 and 2 the cyclic voltammetry results indicate an anion radical sufficiently stable to be characterised by its EPR spectrum, registered under continuous generation at the potential of the first reduction wave. Compound 2 was chosen for the analysis of the spectrum because the presence of the methyl group onto the dibenz-[b,e]-thiepinone moiety facilitates the assignment of the hyperfine splitting constants (hfs). The spectrum obtained for compound 2 is shown in Fig. 4a.

The spectrum is due to the interaction with 7 protons and was simulated (Fig. 4b) with the following hyperfine constants:  $a_{\text{CH3}} = 0.208\,\text{mT},\ a_{\text{H}} = 0.267\,\text{mT},\ a_{\text{H}} = 0.325\,\text{mT},\ a_{\text{2H}} = 0.070\,\text{mT}$  and a line-width  $\delta = 0.087\,\text{mT}$ , indicating an EPR pattern similar to that of the previously investigated unsubstituted derivative (R<sub>2</sub> = H), but with a poorer resolution [8]. The experimental hfs attest for the delocalization of the odd electron on the basic heterocycle and the vinyl moiety, practically not modified by the aryl methoxy substitution.

In the case of compounds **3** and **4** no detectable EPR spectrum was evidenced at the electrochemical reduction in DMSO, in agreement with the lower stability of the anion radical indicated by the cyclic voltammetry data.

#### 3.3. MO calculations

MO calculations were performed in order to get a deeper insight in the reductive pathways of the investigated compounds and to account for the reactivity of the intermediate species, anion radicals and dianions, involved in redox processes in function of their electronic structure. As electrochemical processes imply charged species, and usually take place in highly polar solvents like DMSO, solvation effects are important and can not be neglected in the theoretical modeling. Therefore, solvent dependent PM3 semi empirical calculations using the model of solvation COSMO implemented into AMPAC program package were performed on the starting neutral molecules and the corresponding intermediate species evidenced by the experimental results.

The electronic parameters important in redox processes ( $\epsilon_{\text{HOMO},}$  the energy of the last occupied molecular orbital,  $\epsilon_{\text{LUMO1}}$  and  $\epsilon_{\text{LUMO2}}$  the energies of the first and second vacant orbitals, vertical electronegativities  $X_{\text{v}}$ , adiabatic electron affinities  $EA_{\text{ad}}$ ) calculated in DMSO, are presented in Table 1 together with the

relevant experimental data (E1, and the difference between the first and second reduction steps  $\Delta E_{1,2}^{0}$ ).

It must be noticed, that the experimental data have shown only minor influence of the methyl substitution in the basic heterocycle, reflected in the similar behaviour of compounds 1 and 2, respectively 3 and 4. Therefore, only the results on the unsubstituted derivatives (compounds 1 and 3) will be discussed.

For the sake of comparison, the 6-vinyl thiepin-11-one derivative (T-vinyl-SO<sub>2</sub>) was also calculated and included in Table 1, although no experimental data for this compound are available.

The main statements that emerge from the above results are as follows:

The presence of the R<sub>2</sub> -phenyl group onto the thiepinone vinyl sulfone moiety results in a lower LUMO orbital energy and an increase of the adiabatic electro affinity EA<sub>ad</sub> of compounds 1 and 3 as against T-vinyl-SO<sub>2</sub>.

The higher electro affinity (EA<sub>ad</sub>) and vertical electronegativity, (X,), as well as the lower LUMO position for 3 vs 1 are in agreement with the less negative reduction potential (E,0) experimentally observed for the chloro substituted derivative.

The calculated difference between the first and second LUMO orbitals,  $\Delta \epsilon_{\text{LUMO}}$ , is in agreement with the difference between the potential of the two redox couples in cyclic voltammetry.

The frontier molecular orbitals for compounds 1 and 3 are similar and therefore only HOMO, LUMO and the single occupied molecular orbital in the anion radical (SOMO) of compound 1 are presented in Fig. 5. The highest occupied molecular orbital, HOMO, from which an electron is removed in oxidation processes, is delocalised on the aryl vinyl moiety, indicating that this entity is determinant for the donor properties of the molecule. The first vacant orbital LUMO1, which is singly occupied in the corresponding anion radical, is

mainly localized on the central heterocycle, carbonyl group and on the vinyl fragment, attesting that these structural entities are mainly involved in reduction processes (Fig. 5). The shape of LUMO accounts also for the EPR pattern observed for the anion radical of 1, corresponding to a π-type anion radical, with highest hf splittings for the vinyl proton, followed by positions 2,9 in the benzenic rings of the parent heterocycle.

The influence of the more electronegative chloro substituent R, is reflected, besides the lower  $\epsilon_{\text{LUMO}}$ and higher electro affinity, by the higher reactivity of the anion radical, evidenced by its shorter life time (< 3s for 3 and > 14 s for 1), justifying the ECECE reaction sequence for 3, as against the EECE for 1.

As the nature of the chemical steps following the first and the second ET is concerned, two possibilities are to be considered: (a) Comparison with other halogen aromatic derivatives [21] suggest that the presence of the good leaving group CI may induce a reductive cleavage of the C-Cl bond in the anion radical B., which could account for the chemical step following the first ET for the chloro derivative 3. (b) On another side, literature data on aryl vinyl sulfones [22,23] and on other substituted dibenz -[b,e]-thiepinone derivatives [3-8] suggest the possible reductive cleavage of the C – SO<sub>2</sub> bond. Taking into account the minor differences of the cyclic voltammetry curves in the positive potential range and the similitude of the Digisim parameters accounting for the chemical steps following the second ET of compounds 1 and 3, the second hypothesis seems more probable, and therefore both chemical reactions were tentatively assigned to the reductive cleavage of the C-SO<sub>3</sub> bond in the central ring.

Further support for this assignment is given by the comparison of the shape of the single occupied molecular orbital (SOMO) of the anion radicals and the LUMO of the neutral molecules 1 and 3 in Fig. 5. The differences observed passing from LUMO to SOMO,

Table 1. Calculated redox properties (PM3, DMSO) of the neutral compounds: energies of the frontier molecular orbitals: ε<sub>HOMO1</sub>, ε<sub>LUMO1</sub>, ε<sub>LUM</sub> vertical electronegativities X, adiabatic electro affinities EA<sub>art</sub> difference between the energies of LUMO1 and LUMO2,  $\Delta \epsilon_{\text{LUMO}}$  and the relevant experimental parameters: standard potential of the first reduction wave E<sub>1</sub>°, and difference between the potentials of the first and second reduction steps  $\Delta E_{1,2}^0$ 

| compound                | <sup>8</sup> номо<br>(eV) | E <sub>LUMO1</sub> (eV) | E <sub>LUMO2</sub><br>(eV) | <b>X</b> <sub>V</sub> <sup>(a)</sup><br>(eV) | EA <sub>ad</sub> (b)<br>(eV) | E° <sub>1</sub> (v) | $\Delta arepsilon_{	extsf{LUMO}}$ (eV) | $\Delta \mathbf{E^0}_{	extsf{1-2}}$ (v) |
|-------------------------|---------------------------|-------------------------|----------------------------|--|------------------------------|---------------------|--|---|
| 1                       | -9.468                    | -1.419                  | -0.970                     | 5.44   | 3.55                         | -0.963              | 0.449                                  | 0.487                                   |
| 3                       | -9.521                    | -1.481                  | -1.024                     | 5.50   | 3.69                         | -0.921              | 0.457                                  | 0.489                                   |
| T-vinyl-SO <sub>2</sub> | -9.914                    | -1.223                  | -0.754                     | 5.56   | 3.37                         | -                   | 0. 469                                 | -                                       |

<sup>(</sup>a)  $X_{a} = -1/2$  ( $\varepsilon_{HOMO} + \varepsilon_{LUMO}$ )
(b)  $EA_{ad} = H_A^i - H_A^i$ , where the  $H_A^i$  is the enthalpy of formation at the optimized geometry of the neutral molecule and the  $H_A^i$  is the enthalpy of formation at the optimized geometry of the anion radical [21,22]

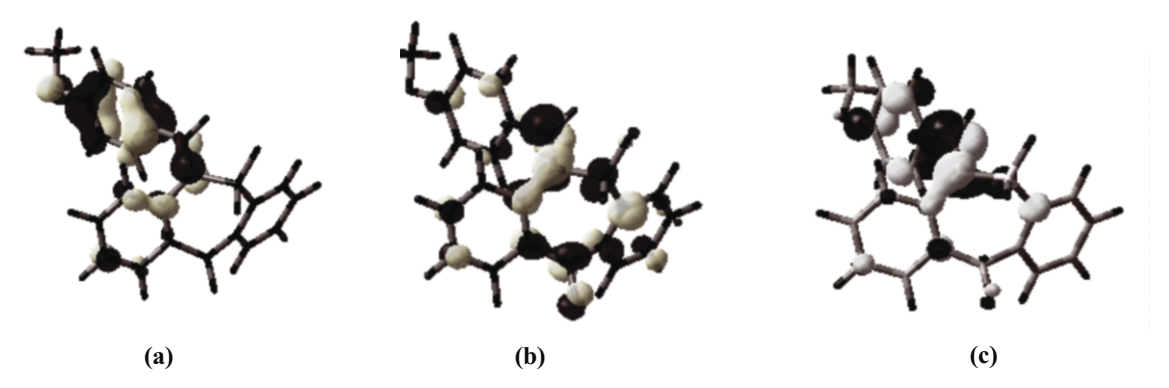


Figure 5. Shape of HOMO (a) and LUMO (b) at the optimized geometry of the neutral molecule, and SOMO (c) at the optimized geometry of the anion radical of compound 1

Table 2. Calculated bond orders of the C<sub>vin</sub> – SO<sub>2</sub> and C<sub>ar</sub> – SO<sub>2</sub> bonds (PM3; DMSO) at the equilibrium geometry of the neutral compounds, anion radicals and dianions of 1, 3, and T-vinyl-SO<sub>2</sub>

| Compound                | Neutral n                          | nolecule                         | Anion r                            | adical                           | Dianion                           |                                  |  |
|-------------------------|------------------------------------|----------------------------------|------------------------------------|----------------------------------|-----------------------------------|----------------------------------|--|
|                         | C <sub>vin</sub> - SO <sub>2</sub> | C <sub>ar</sub> -SO <sub>2</sub> | C <sub>vin</sub> - SO <sub>2</sub> | C <sub>ar</sub> -SO <sub>2</sub> | C <sub>vin</sub> -SO <sub>2</sub> | C <sub>ar</sub> -SO <sub>2</sub> |  |
| 1                       | 0.760                              | 0.759                            | 0.899                              | 0.711                            | 0.895                             | 0.712                            |  |
| 3                       | 0.756                              | 0.760                            | 0.897                              | 0.715                            | 0.906                             | 0.710                            |  |
| T-vinyl-SO <sub>2</sub> | 0.766                              | 0.761                            | 0.713                              | 0.880                            | 0.730                             | 0.935                            |  |

consisting in a decrease of the electron density on the carbonyl group and basic heterocycle, simultaneously with an increase in the vinyl sulfone bond, are specific to the dissociative electron transfer (DET) [7,8,25,26]. These changes are assigned to the formation in the first step of a "stiff" anion radical, in our case the  $\pi$ -type anion radical mainly associated with the reduction of the carbonyl group. Its formation needs only small molecular deformation as against the neutral molecule, is characterised by a low intrinsic barrier, and is reflected in the shape of LUMO, mainly delocalised on the basic heterocycle and the vinyl group, both C-S bonds having an antibonding character. The shape of SOMO in Fig. 5 suggests a higher contribution of a "looser" structure of the anion radical, in which the odd electron is also localised in an antibonding  $(\sigma^*)$  molecular orbital of the bond undergoing cleavage, namely the C<sub>ar</sub> – SO<sub>3</sub> bond. This is in agreement with a relatively high intrinsic barrier for the ET steps, reflected in the low k values  $(\sim 10^{-3} \text{ cm s}^{-1}).$ 

Information regarding the regioselectivity of the bond breaking can be furnished by the evolution of the bond orders for  $C_{\text{vin}}$  -  $SO_2$  and  $C_{\text{ar}}$  -  $SO_2$  bonds in the corresponding neutral molecules, anion radicals and dianions, calculated and presented in Table 2.

A decrease of the  $\mathrm{C_{ar}} - \mathrm{SO_2}$  bond order was observed passing from the neutral molecule to the corresponding anion radical and dianion for compounds **1** and **3** (Table **2**) and, at the same time, an increase of the

 $C_{vin}$  -  $SO_2$  bond order, suggesting the possible cleavage of the  $C_{ar}$  - S bond during the reduction process. For **T-vinyl-SO**<sub>2</sub> a reverse order of cleavage is evidenced by the results in Table 2. It can be supposed that this type of regioselectivity of the C-S bond cleavage passing from compounds 1 and 3 to **T-vinyl-SO**<sub>2</sub> is due to the presence in molecule of the R<sub>2</sub>-phenyl group.

### 4. Conclusions

Four derivatives of aryl vinyl dibenz [b,e]-thiepin-5,5-dioxide-11-one, differing in the heterocycle substituent R1 and/or the vinyl-aryl substituent R2 were investigated by cyclic and linear voltammetry with stationary and rotating disc electrode (RDE) aided by digital simulations, coupled with EPR spectroelectrochemistry. The experimental results outline the minor influence of the methyl substitution in the parent heterocycle  $R_{\rm 1}$ , and a different reduction mechanism in function of the substituent in the arylvinyl moiety  $R_{\rm 2}$ .

The EECE reaction sequence proposed for compounds 1 and 2 accounts for a relatively stable anion radical, characterised by EPR spectroelectroelectrochemistry, whereas the higher reactivity of the anion radical formed as a result of the first ET for compounds 3 and 4 shows that an ECECE sequence is more probable for these derivatives.

The solvent dependent PM3-MO-calculations, using the dielectric continuum model implemented into the AMPAC program package, account reasonably well for the higher reducibility of the chloro substituted compounds, as well as for the higher reactivity of the radical anions of **3** and **4** in comparison with **1** and **2**. The higher electro affinity (EA $_{ad}$ ) and vertical electronegativity, (X $_{v}$ ), as well as the lower LUMO position for **3** vs **1** are in agreement with the less negative reduction potential (E $_{1}^{0}$ ) experimentally observed for the chloro substituted derivatives.

The decrease of the  $C_{ar} - SO_2$  bond order observed passing from the neutral molecule to the corresponding anion radical and dianion for all compounds and, at the

same time, an increase of the  $\rm C_{vin}$  -  $\rm SO_2$  bond order, suggest the possible cleavage of the  $\rm C_{ar}$ -S bond during reduction process.

Although not all intermediate species could be identified, the present approach, using electrochemical and EPR techniques and Digisim simulations, coupled with solvent dependent semiempirical MO calculations can account for the main features of the reduction mechanism of the four substituted aryl vinyl thiepinone derivatives investigated in this work.

#### References

- [1] M. Rajsner, J. Metsy, E. Svatek, M. Protiva, Collect. Czech. Chem. Commun. 34, 1015 (1969)
- [2] M. Rajsner, M. Protiva, Patent No. CS 143379 CS 1968-7190
- [3] E. Volanschi, C. Vladescu, C. Volansci, Rev. Roum. Chim. 19, 755 (1974)
- [4] M. Ciureanu, M. Hillebrand, E. Volanschi J. Electroanal. Chem. 291, 201 (1990)
- [5] M. Ciureanu, M. Hillebrand, E. Volanschi,J. Electroanal. Chem. 322, 221 (1992)
- [6] M. Ciureanu, M. Hillebrand, E. Volanschi, J. Mol. Struct. 294, 267 (1993)
- [7] E. Volanschi, S.H. Suh, M. Hillebrand, J. Electroanal. Chem. 602, 181 (2007)
- [8] L. Preda, V. Lazarescu, M. Hillebrand, E. Volanschi, Electrochem. Acta 51, 5587 (2006)
- [9] EPR Simulation Program for Windows, http://epr.niehs.nih.gov/pest.html
- [10] A. Klamt, G. Schüürmann, J. Chem. Soc., Perkin Trans 2, 799 (1993)
- [11] C.P. Andrieux, J.M. Saveant, In: C.F. Bernasconi (Ed.), Investigations of rates and mechanisms of reactions (Wiley, New York, 1986), vol.6, 4/E, Part 2, 305
- [12] A.J. Bard, L.R. Faulkner, Electrochemical Methods. Fundamentals Applications, 2nd edition (Wiley, New York, 2001)
- [13] L. Nadjo, J.M. Saveant, Electroanal. Chem. And Interfacial Electrochem. 48, 113 (1973)
- [14] C.P. Andrieux, A. Le Gorand, J.M. Saveant, J. Am. Chem. Soc. 114, 6892 (1992)

- [15] P. Cauliez, M. Benaskar, A. Ghanimi, J. Simonet, New J. Chem. 253 (1998)
- [16] J.F. Pilard, O. Fourets, J. Simonet, L.J. Klein, D.G. Peters, J. Electrochem. Soc. 148, E171 (2001)
- [17] A. Ghanimi, J. Simonet, J. Electroanal. Chem. 425, 217 (1997)
- [18] J. Delaunay, G. Mabon, M. Chaquiq El Badre, A. Orliac, J. Simonet, Tetrahedron Letters 33, 2149 (1992)
- [19] L.J. Klein, D.G. Peters, O. Fourets, J. Simonet, J. Electroanal. Chem. 487, 66 (2000)
- [20] A. Botrel, E. Furet, O. Fourets, J.F. Pilard, New J. Chem. 24, 815 (2000)
- [21] J.M. Saveant, J. Am. Chem. Soc. 114, 10595 (1992)
- [22] J. Simonet, In: S. Patai, Z. Rappoport, C.J.M. Stiriling (Eds.), The Chemistry of Sulphur-Containing Functional Group (Wiley, NY, 1998)
- [23] J. Simonet, In: S. Patai, Z. Rappoport, C.J.M. Stiriling (Eds.), The Chemistry of Sulphur-Containing Functional Group (Wiley, NY, 1998)
- [24] A. Sawyer, E. Sullivan, Y.H. Mariam, J. Comput. Chem. 17, 204 (1996)
- [25] A.B. Meneses, S. Antonello, M.C. Arevalo, F. Maran, Electrochem. Acta 50, 1207 (2005)
- [26] J. M. Saveant, in: D. Bethel (Ed.), Single electron transfer and nucleophilic substitution in Advances in Organic Chemistry (Academic Press Ed., NY, 1990) vol 26, 17